

Cannabinoid receptor 1 (CB1) antagonism enhances glucose utilisation and activates brown adipose tissue in diet-induced obese mice

M. Bajzer · M. Olivieri · M. K. Haas · P. T. Pfluger ·
I. J. Magrisso · M. T. Foster · M. H. Tschöp ·
K. A. Krawczewski-Carhuatanta · D. Cota · S. Obici

Received: 30 May 2011 / Accepted: 10 August 2011 / Published online: 11 October 2011
© Springer-Verlag 2011

Abstract

Aims/hypothesis We examined the physiological mechanisms by which cannabinoid receptor 1 (CB1) antagonism improves glucose metabolism and insulin sensitivity independent of its anorectic and weight-reducing effects, as well as the effects of CB1 antagonism on brown adipose tissue (BAT) function.

Methods Three groups of diet-induced obese mice received for 1 month: vehicle; the selective CB1 antagonist SR141716; or vehicle/pair-feeding. After measurements of body composition and energy expenditure, mice underwent euglycaemic–hyperinsulinaemic clamp studies to assess in vivo insulin action. In separate cohorts, we assessed insulin action in weight-reduced mice with diet-induced obesity (DIO), and the effect of CB1 antagonism on BAT thermogenesis. Surgical denervation of interscapular BAT (iBAT) was carried out in order to study the requirement for the sympathetic nervous system in mediating the effects of CB1 antagonism on BAT function.

Results Weight loss associated with chronic CB1 antagonism was accompanied by increased energy expenditure, enhanced insulin-stimulated glucose utilisation, and marked activation of BAT thermogenesis. Insulin-dependent glucose uptake was significantly increased in white adipose tissue and BAT, whereas glycogen synthesis was increased in liver, fat and muscle. Despite marked weight loss in the mice, SR141716 treatment did not improve insulin-mediated suppression of hepatic glucose production nor increase skeletal muscle glucose uptake. Denervation of iBAT blunted the effect of SR141716 on iBAT differentiation and insulin-mediated glucose uptake.

Conclusions/interpretation Chronic CB1 antagonism markedly enhances insulin-mediated glucose utilisation in DIO mice, independent of its anorectic and weight-reducing effects. The potent effect on insulin-stimulated BAT glucose uptake reveals a novel role for CB1 receptors as regulators of glucose metabolism.

Keywords Brown adipose tissue · CB1 receptors · Diet-induced obesity · Euglycaemic–hyperinsulinaemic clamp · Glucose utilisation · Obesity · Rimonabant · SNS denervation · SR141716

M. Bajzer and M. Olivieri contributed equally to this work.

Electronic supplementary material The online version of this article (doi:10.1007/s00125-011-2302-6) contains peer-reviewed but unedited supplementary material, which is available to authorised users.

M. Bajzer · M. Olivieri · M. K. Haas · P. T. Pfluger ·
I. J. Magrisso · M. T. Foster · M. H. Tschöp ·
K. A. Krawczewski-Carhuatanta · S. Obici (✉)
Metabolic Diseases Institute, University of Cincinnati,
2140 East Galbraith Road, Building B, Room 332,
Cincinnati, OH 45237-1625, USA
e-mail: silvana.obici@uc.edu

D. Cota
Inserm U862, Neurocentre Magendie, University Bordeaux,
Bordeaux, France

Abbreviations

CB1	Cannabinoid receptor 1
BAT	Brown adipose tissue
DIO	Diet-induced obesity
iBAT	Interscapular BAT
PF	Vehicle-treated and pair-fed with the average amount of food ingested by the SR group during the previous day
SNS	Sympathetic nervous system
SR	SR141716-treated with unlimited access to food
VEH	Vehicle-treated with unlimited access to food
WAT	White adipose tissue

Introduction

The endocannabinoid system has emerged as a key player in both the central and peripheral control of energy balance and glucose metabolism. Chronic pharmacological interventions with selective inhibitors of cannabinoid receptor 1 (CB1), such as rimonabant (SR141716), leads to decreased adiposity as the result of both reduced food intake and increased energy expenditure. The latter mechanism plays a larger role in the weight-loss effects of these drugs, as demonstrated by pair-feeding studies [1, 2]. Mice null for *Cb1* (also known as *Cnr1*) display reduced body weight, adiposity, resistance to diet-induced obesity (DIO), and improvement in glucose regulation [3]. These results implicate the CB1 receptors and its intracellular signalling as critical modulators of energy balance and glucose metabolism.

Despite clear evidence that pharmacological CB1 antagonism improves insulin sensitivity [1, 4–7], the specific mechanisms are still under investigation. In particular, it is still unclear how chronic CB1 antagonism improves insulin sensitivity and what tissues are its target of action. In this regard, the brown adipose tissue (BAT) has emerged as an important modulator of energy expenditure and glucose utilisation [8, 9]. The notion that adult humans do not retain functional BAT has been dispelled by recent evidence, which points to BAT as an important player in the pathogenesis of obesity and diabetes [10–12]. Notably, pharmacological blockade or genetic ablation of CB1 has been linked to the activation of the BAT, which further underscores the role of this tissue as a potential target for obesity and diabetes therapy [8].

In this report, we examine the effects of CB1 antagonism on glucose metabolism and insulin sensitivity, independent of its effects on food intake and adiposity. Since CB1 antagonism activates BAT thermogenesis and glucose uptake, we investigated whether these effects require an intact sympathetic nervous system (SNS).

Methods

Mice

All animal protocols were approved by the University of Cincinnati Institutional Animal Care and Use Committee. Nine-week-old C57BL/6 J male mice (Jackson Laboratories, Bar Harbor, ME, USA) were housed in temperature-controlled rooms (21–23°C) with a 12 h light–dark cycle, and fed with a 60% high-fat diet (D12492, Research Diets, New Brunswick, NJ, USA) for 1 month.

Energy balance and euglycaemic–hyperinsulinaemic clamp studies DIO mice were randomised into three groups

($n=11$ /group): vehicle-treated with unlimited access to food (VEH); SR141716-treated with unlimited access to food (SR); and vehicle-treated and pair-fed with the average amount of food ingested by the SR group during the previous day (PF). Mice were injected daily i.p. and fed 1 h before lights out for 7 weeks. Body composition by quantitative magnetic resonance (Echo MRI Whole Body Composition Analyzer, Echo Medical Systems, Houston, TX, USA) and indirect calorimetry (TSE Systems, Chesterfield, MO, USA) were performed after 4 weeks of treatment. Euglycaemic–hyperinsulinaemic clamp experiments were carried out after 5–6 weeks of treatment.

BAT denervation studies The interscapular BAT (iBAT) of DIO mice was surgically denervated or sham-operated. After recovery, each group was randomised to receive SR or vehicle ($n=13$ –15/group). Mice were injected daily i.p. 1 h before lights out for 8 weeks. All mice had unlimited access to food and water. Food intake and body weight were recorded daily. Body composition analysis by MRI and indirect calorimetry were performed after 6 weeks of treatment and glucose uptake after 8–9 weeks of treatment.

BAT thermogenesis studies DIO mice were implanted with temperature probes (see methods in the electronic supplementary material [ESM]) or sham-operated. After recovery, the mice received vehicle or SR ($n=6$ /group). Mice were injected i.p. daily 4 h before lights out. BAT temperature was measured every 30 min from 11:00 hours to 19:00 hours for 12 days. Afterwards, mice were implanted with a jugular catheter and, upon recovery, were injected with a bolus of 2-deoxy-D-[U-¹⁴C]glucose (370 kBq) to measure basal glucose uptake in BAT. All mice had unlimited access to food and water.

Food-restricted euglycaemic–hyperinsulinaemic clamp studies Ten-week-old C57bl/6 mice from Jackson Laboratories were fed a low-fat standard chow or a 60% high-fat diet (D12492, Research Diets) for 5–6 weeks. DIO mice were divided into two groups receiving a high-fat diet that was either unlimited or restricted to 85% of the unlimited food intake. After 5 weeks, mice underwent surgical implantation of jugular catheters and, after recovery, underwent euglycaemic–hyperinsulinaemic clamp studies ($n=5$ /group).

Drug studies

SR141716 was obtained from the NIMH Chemical Synthesis and Drug Supply Program (www.nimh-repository.rti.org), and administered i.p. at 10 mg/kg daily in all studies. This dose has been previously used i.p. and by mouth to similar effect [9, 13, 14]. A 1 mg/ml emulsion of SR141716 was

made by dissolving 100 mg of SR141716 in 1 ml DMSO. Next, 2 ml of Tween 80 was added while vortexing. Finally, 97 ml of saline was slowly added while vortexing.

Euglycaemic–hyperinsulinaemic clamp studies and glucose uptake in skeletal muscle

Euglycaemic–hyperinsulinaemic clamp studies were performed in conscious, chronically catheterised mice, as described by Okamoto et al. and Lo et al. [15, 16]. Briefly, during the clamp studies, which lasted for 90 min, we infused a solution of glucose (20% wt/vol.) at a variable rate as required to maintain euglycaemia. Mice received primed-constant infusions of [$^3\text{-}^3\text{H}$]glucose (bolus of 74 kBq followed by 3.7 kBq/min; NET-331 C, Perkin Elmer, Boston, MA, USA) and insulin (bolus of 88 mU/kg followed by 5 mU $\text{min}^{-1} \text{kg}^{-1}$; Humulin R, Eli Lilly, Indianapolis, IN, USA).

We collected plasma samples to determine glucose concentrations and tracer-specific activities at times 0, 30, 50, 60, 70, 80 and 90 min. Additional sample volumes were taken at 0, 60 and 90 min to determine basal and clamped insulin levels and NEFA. To measure tissue-specific glucose uptake, we injected a bolus (370 kBq) of 2-deoxy-D-[U- ^{14}C]glucose at time=45 min. At the end of the clamp studies, mice were killed and tissue samples were quickly harvested and stored at -80°C for further analysis.

Indirect calorimetry

Indirect calorimetry was performed as described by Pfluger et al. [17]. Mice were individually housed in metabolic chambers (TSE Systems) in which fluid, food intake, locomotor activity and gas exchanges can be monitored. Following 48 h of acclimatisation, O_2 consumption, CO_2 production and locomotor activity were measured every 6 min for a total of 72 h to measure the gas exchange, respiratory quotient and energy expenditure. Energy expenditure values were normalised to the body weight of the animals. Home-cage locomotor activity was determined using a tri-dimensional infrared light beam system and expressed as beam breaks/24 h.

Western blot

Tissue was homogenised using the Qiagen TissueLyser bead mill (Qiagen, Valencia, CA, USA). Proteins were extracted with RIPA buffer (150 mmol/l NaCl, 1.0% [vol./vol.] Triton X-100, 0.5% [wt/vol.] sodium deoxycholate, 0.1% [vol./vol.] SDS, 50 mmol/l Tris, pH 8.0) and then centrifuged for 10 min at 10,000g. A 30 μg sample of protein was separated on a 10% Tris-HCl gel and transferred to polyvinylidene-fluoride membrane for 1 h at

4°C at 100 V. The membrane was blocked with 5% (wt/vol.) non-fat dry milk in Tris-buffered saline with Tween 20 for 1 h at room temperature, followed by 1:1,000 dilution of tyrosine hydroxylase antibody (catalogue identifier ab152, Millipore, Billerica, MA, USA) overnight at 4°C with a 1:10,000 dilution of goat anti-rabbit secondary antibody (Abcam, Cambridge, MA, USA) for 1 h at room temperature. Bands were visualised using the Pierce ECL western blotting substrate (catalogue identifier 32106, Thermo Scientific, Rockford, IL, USA).

Analytical procedures and calculations

Plasma glucose was measured by the glucose oxidase method in a GM7 Analyser (Analox Instruments USA, Lunenburg, MA, USA). The rate of glycolysis was determined by measuring the tritium on the C-3 position of our glucose tracer that is lost into water during glycolysis [18]. Thus, the plasma tritium is present in two chemical forms: ^3H -labelled water or [$^3\text{-}^3\text{H}$]glucose. To measure both forms, we counted radioactivity in plasma samples deproteinised with $\text{Ba}(\text{OH})_2$ and ZnSO_4 , before and after each sample was evaporated to dryness. The dry counts represent plasma [$^3\text{-}^3\text{H}$]glucose, whereas the difference between the wet and dry counts is a measure of the tritiated water.

Under steady-state conditions for plasma glucose, the rate of glucose disposal (R_d) is assumed to be equal to the rate of glucose appearance (R_a). We determined R_d by dividing the infusion rate for [$^3\text{-}^3\text{H}$]glucose (disintegrations/min) by the specific activity of plasma [$^3\text{-}^3\text{H}$]glucose (disintegrations $\text{min}^{-1} [\text{mg glucose}]^{-1}$). The rate of glucose production is calculated as the difference between R_d and the rate of glucose infusion.

The tissue-specific rate of glycogen synthesis was quantified by measuring the rate of incorporation of [$^3\text{-}^3\text{H}$]glucose into glycogen. Tissue glycogen concentrations were determined after digestion with amyloglucosidase, as described by Massillon et al. and Rossetti et al. [18, 19]. The glycogen synthetic rate was obtained by dividing the [$^3\text{-}^3\text{H}$]glucose radioactivity in glycogen (disintegrations $\text{min}^{-1} [\text{g tissue}]^{-1}$) by the mean specific activity of [$^3\text{-}^3\text{H}$]glucose in plasma during the insulin clamp (disintegrations $\text{min}^{-1} [\mu\text{g plasma glucose}]^{-1}$).

To measure the tissue-specific rate of glucose uptake we weighed and dissolved tissues in 0.5 ml of 1 mol/l NaOH, and incubated them in a shaking water bath at 60°C for 1 h. After neutralisation with 0.5 ml of 1 mol/l HCl, two aliquots were taken. One was deproteinised with $\text{Ba}(\text{OH})_2$ and ZnSO_4 and the other with a 6% solution of HClO_4 . The HClO_4 supernatant fraction contained both phosphorylated and unphosphorylated 2-deoxyglucose, whereas the $\text{Ba}(\text{OH})_2$ and ZnSO_4 supernatant fraction contained only

the unphosphorylated form. The difference in counts between the two supernatant fractions is a measure of the tissue content of 2-deoxy-[U-¹⁴C]glucose 6-phosphate.

The rate of tissue glucose uptake was obtained by dividing the tissue content of 2-deoxy-[U-¹⁴C]glucose 6-phosphate by the specific activity of 2-deoxy-[U-¹⁴C]glucose in plasma [19]. Plasma insulin and leptin were measured with a MILLIPLEX MAP Mouse Serum Adipokine Panel (catalogue identifier MADPK-71 K, Linco Research, St Charles, MO, USA). Plasma adiponectin was measured with MILLIPLEX MAP Mouse Adipocyte Panel (catalogue identifier MADPCYT-72 K, Millipore). NEFA in plasma was measured with a kit from Waco Pure Chemical Industries (Osaka, Japan).

iBAT denervation

Mice were anaesthetised with isoflurane and a transverse incision was made in the skin anterior to the iBAT fat pads. The pads were identified and separated from the underlying muscle by blunt dissection. Four intercostal nerve bundles entering each fat pad were identified, and a section of each nerve bundle was removed bilaterally. Extra care was taken to ensure that the blood supply was not disrupted.

Statistical analysis

Statistical analysis was performed using GraphPad Prism (GraphPad Software, La Jolla, CA, USA). One-way ANOVA with Bonferroni post hoc test was used to determine significance at ($p \leq 0.05$) for studies involving pair-feeding. Denervation studies were analysed using a two-way ANOVA with Bonferroni post hoc test for significance ($p \leq 0.05$). All time course studies were analysed by two-way ANOVA with repeated measures and Bonferroni post hoc test ($p \leq 0.05$).

Results

CB1 antagonism reduces adiposity and increases energy expenditure in DIO mice

To determine the effects of chronic CB1 antagonism on energy balance and body composition, DIO mice received daily i.p. injections of SR141716 for 4 weeks or its vehicle, or were pair fed according to the intake of the SR group for the same length of time. SR treatment elicited a profound but transient reduction in food intake (Fig. 1a), which is consistent with the rapid weight loss achieved in the first few days of SR treatment and pair-feeding [1, 2]. However, pair-feeding alone was insufficient to attain the same weight loss as the SR group (Fig. 1b). The fat mass of

DIO mice was significantly reduced in the SR group compared with the VEH and PF groups, suggesting that the loss of adiposity with CB1 antagonism is mediated by increased energy expenditure (Fig. 1c, d). Indeed, energy expenditure measured by indirect calorimetry was increased in the SR group compared with both VEH and PF groups (Fig. 1e), and was not due to increased locomotor activity (Fig. 1f). As expected in DIO mice consuming a high-fat diet, the respiratory quotient was very low and unchanged in all groups (VEH, 0.75 ± 0.008 ; PF, 0.74 ± 0.008 ; SR, 0.74 ± 0.008). Consistent with the changes in fat mass, plasma leptin levels were significantly decreased by SR141716 treatment, but not by pair-feeding (Table 1).

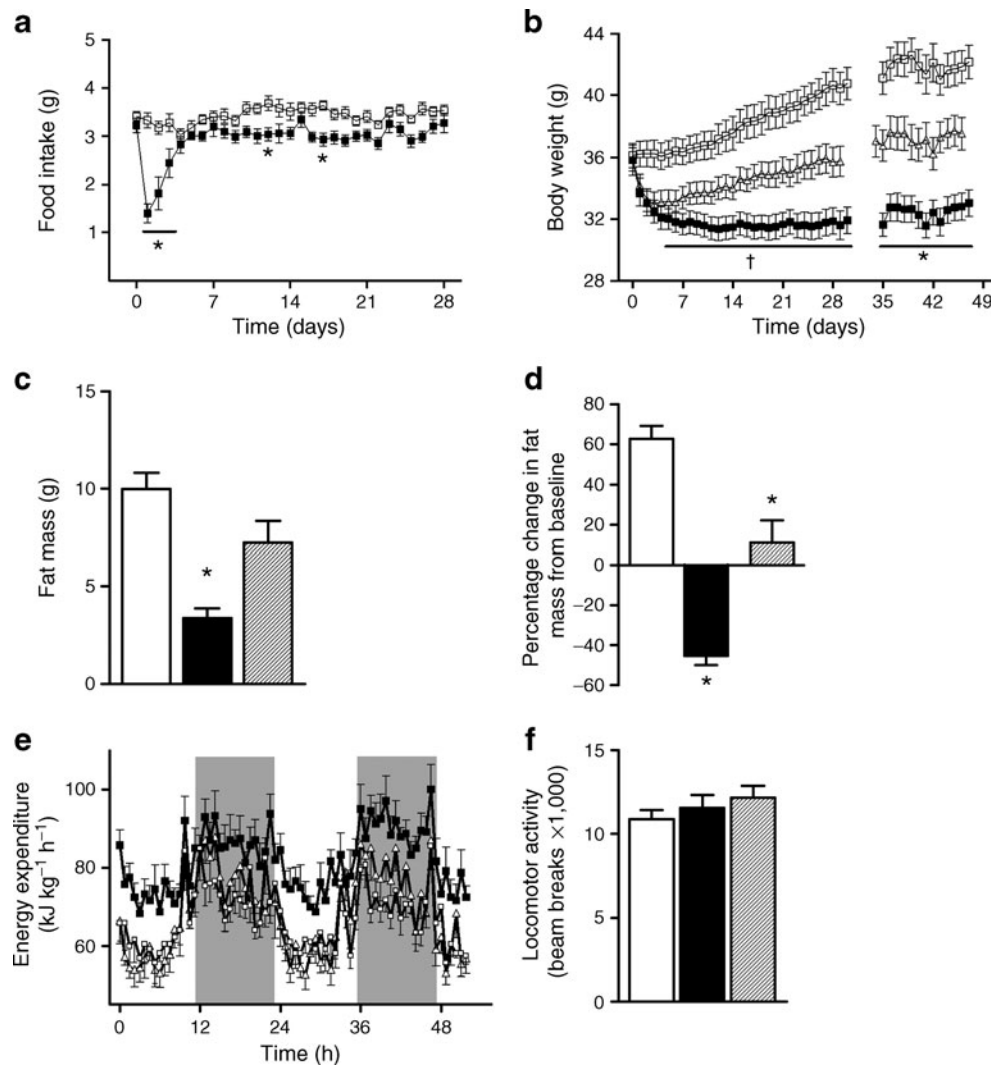
CB1 antagonism increases whole-body insulin-dependent glucose utilisation

SR-induced weight loss was accompanied by a reduction in fasting plasma glucose and insulin levels (Table 1), suggesting improved insulin sensitivity. Fasting levels of adiponectin, triacylglycerols and NEFA were not changed. However, insulin-dependent suppression of plasma NEFA was restored selectively in the SR group (Table 1).

To determine the effects of CB1 antagonism on in vivo insulin action independent of food intake, we performed euglycaemic–hyperinsulinaemic clamp studies in the SR, VEH and PF groups. Glucose infusion rate was significantly higher in the SR group compared with the VEH or PF groups, indicating that CB1 antagonism significantly improves whole-body insulin sensitivity (Fig. 2a). This effect was due to an increase in glucose disposal rate (Fig. 2b). However, the rate of glucose production was not changed among the three groups (Fig. 2c), and neither was the expression of the genes encoding the hepatic gluconeogenic enzymes phosphoenolpyruvate carboxykinase and glucose-6-phosphatase (data not shown), indicating that weight loss induced by SR141716 does not improve hepatic insulin resistance of DIO mice. Consistent with an increased glucose utilisation, SR141716 increased the whole-body glycolysis rate (Fig. 2d).

In order to identify the target tissues for an SR141716-induced increase in glucose utilisation, we measured in vivo glucose uptake in fat and skeletal muscle under hyperinsulinaemic conditions. Glucose uptake in white adipose tissue (WAT; Fig. 2e) and BAT (Fig. 2f) was significantly stimulated by SR141716. In particular, CB1 antagonism stimulated the uptake of glucose in BAT by more than threefold in the SR group compared with the VEH and PF groups (Fig. 2f). In a separate cohort of mice treated with SR141716 or vehicle, we measured in vivo BAT glucose uptake under basal conditions and found no significant difference (31.9 ± 3.9 mg kg⁻¹ min⁻¹ and 45.1 ± 7.0 mg kg⁻¹ min⁻¹ for the VEH and SR groups,

Fig. 1 Energy balance and body composition in DIO C57BL/6 mice treated with 10 mg/kg SR i.p. or vehicle. After 4 weeks of treatment mice were moved to indirect calorimetry cages for 4 days. **a** Food intake and **(b)** body weight of VEH (white squares), PF (triangles) and SR (black squares) mice. **c** Fat mass and **(d)** percentage change in fat mass from baseline of VEH (white bars), PF (hatched bars) and SR (black bars) mice measured by MRI. **e** Energy expenditure and **(f)** locomotor activity were measured by indirect calorimetry cages equipped with a beam-break measurement system. In all groups, $n=11$; $*p<0.05$ SR group vs PF and VEH groups; $†p<0.05$ SR group vs VEH group only



respectively; $n=6/\text{group}$, $p>0.05$). The lack of an increase in BAT glucose uptake under basal conditions suggests that the effect of SR141716 on BAT glucose uptake is mediated by improved insulin sensitivity.

Despite the marked increase in whole-body glucose uptake, the SR group did not display a significant increase in the rate of insulin-stimulated glucose uptake in skeletal muscle (Fig. 3a). However, the rate of insulin-dependent

Table 1 Plasma measurements during fasting and clamp studies in animals treated with vehicle or 10 mg/kg SR i.p., or pair fed for 8 weeks ($n=11/\text{group}$)

Variable	Plasma values		
	VEH group	SR group	PF group
Fasting			
Glucose (mmol/l)	11.5±0.44	9.00±0.50*	9.8±0.39*
Insulin (pmol/l)	136.5±24.5	64.8±8.8*	78.8±12.3
NEFA (mmol/l)	1.07±0.05	1.33±0.09*	1.16±0.08
TAG (mmol/l)	0.659±0.03	0.676±0.04	0.715±0.03
Leptin (ng/ml)	7.6±1.5	1.1±0.3*†	5.0±1.4
Adiponectin (µg/ml)	21.8±1.4	18.4±1.5	18.7±1.6
Clamp			
Glucose (mmol/l)	8.7±0.33	8.5±0.22	8.4±0.39
Insulin (pmol/l)	434.0±50.75	325.5±43.75	330.8±33.25
NEFA (mmol/l)	0.76±0.05	0.49±0.04*	0.67±0.06

* $p<0.05$ vs VEH group;
 $†p<0.05$ vs PF group
 TAG, triacylglycerol

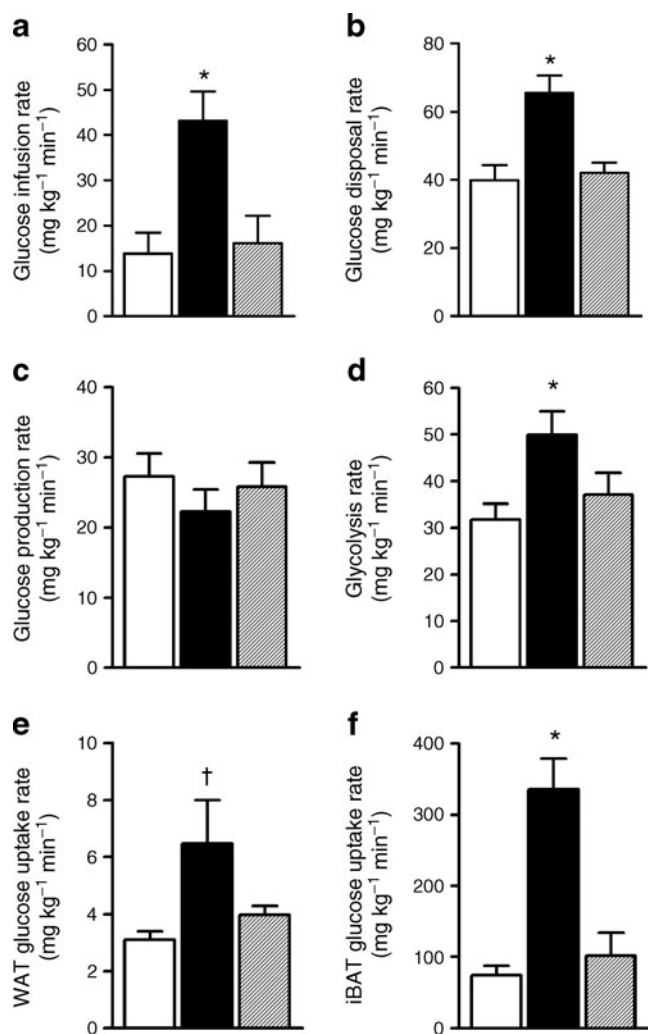


Fig. 2 Hyperinsulinaemic–euglycaemic clamp studies. After 7 weeks of treatment with VEH (white bars), PF (hatched bars) and SR (black bars), mice underwent a hyperinsulinaemic–euglycaemic clamp. Graphs show: **(a)** glucose infusion rate; **(b)** glucose disposal rate; **(c)** glucose production rate; **(d)** whole-body glycolysis rate. Glucose uptake was measured by 2-deoxy-[U- ^{14}C]glucose in WAT **(e)** and iBAT **(f)**. In all groups, $n=11$. * $p<0.05$ SR group vs PF and VEH groups; † $p<0.05$ SR group vs VEH group only

glycogen synthesis was markedly and significantly elevated in skeletal muscle as well as in WAT and liver (Fig. 3b). Notably, pair-feeding was insufficient to elicit any improvement in insulin-dependent glucose metabolism (Figs 2 and 3).

To determine whether chronic CB1 antagonism improved insulin sensitivity via its effect on fat mass reduction, we induced weight loss in DIO mice by food restriction to match the weight reduction achieved with SR141716. We then subjected these mice to euglycaemic–hyperinsulinaemic clamp studies (ESM Fig. 1). Despite reduced adiposity, food-restricted DIO mice did not have improved insulin sensitivity compared with DIO mice that had unrestricted access to food (ESM Fig. 1). Thus, CB1 antagonism improves insulin sensitivity independent of its ability to reduce adiposity.

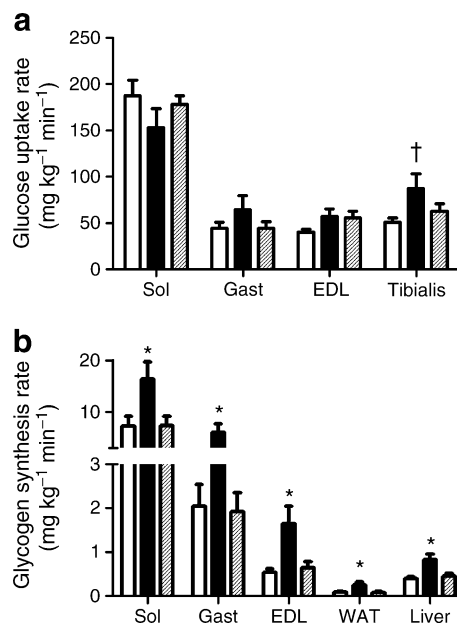


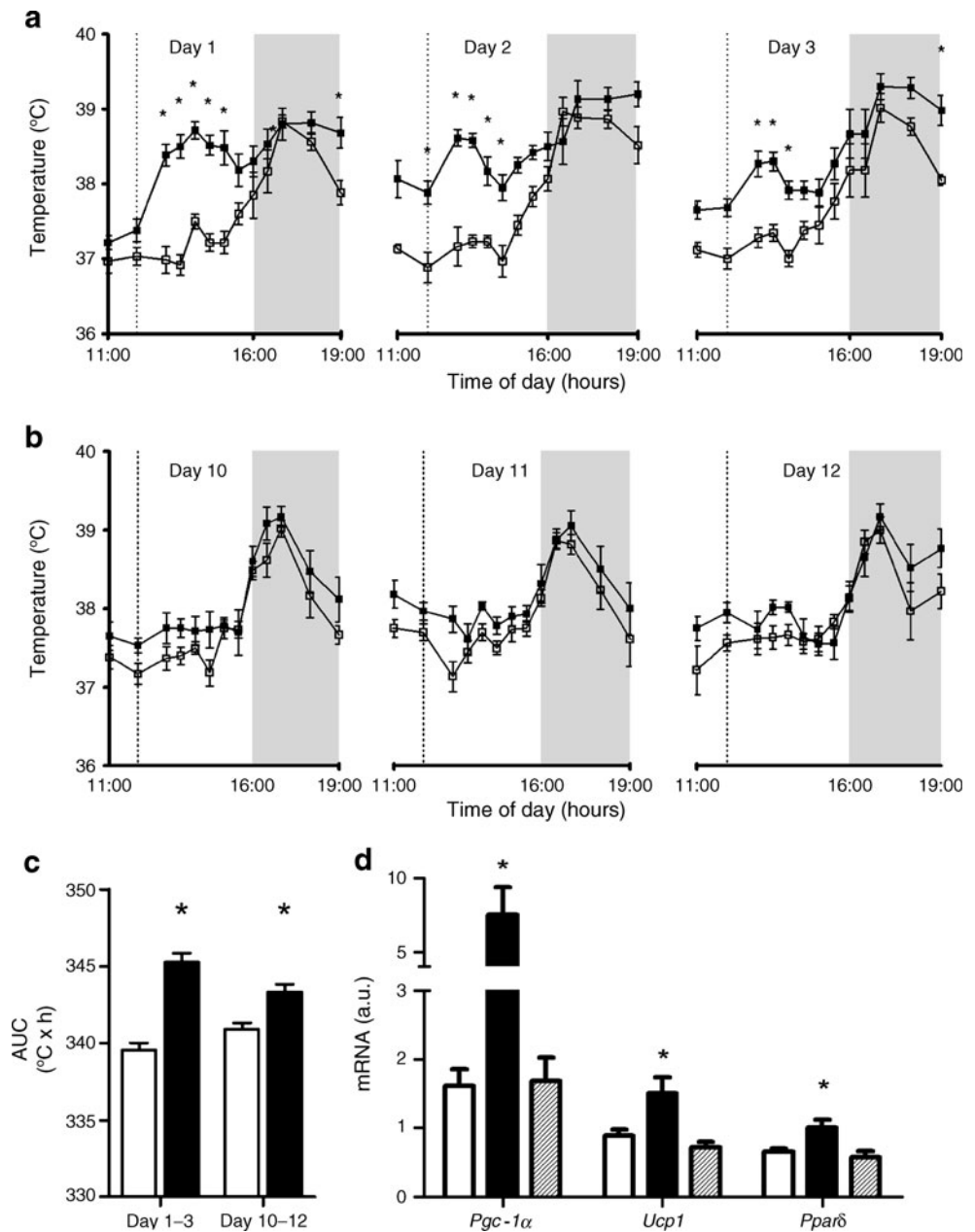
Fig. 3 Rate of tissue glucose uptake and glycogen synthesis. **a** Glucose uptake in several muscles measured by 2-deoxy-[U- ^{14}C]glucose. **b** Glycogen synthesis rate in several muscles, liver and WAT in VEH (white bars), PF (hatched bars) and SR (black bars) groups. In all groups, $n=11$. EDL, extensor digitorum longus; Gast, gastrocnemius; Sol, soleus. * $p<0.05$ SR group vs PF and VEH groups; † $p<0.05$ SR group vs VEH group only

CB1 antagonism activates BAT

The marked increase in glucose utilisation in BAT suggested that CB1 antagonism could exert weight-reducing and insulin-sensitising effects via stimulation of BAT function. Therefore, we tested the ability of SR141716 to activate the BAT function of DIO mice by measuring the temperature of iBAT pads using thermal probes [20]. Temperature-sensing transponders were surgically implanted underneath the iBAT of DIO mice. After recovery, baseline BAT temperatures were recorded every 30 min or hourly from 11:00 to 19:00 hours, across the transition from light to dark in the light–dark cycle (Fig. 4a–c). Then, mice were randomised to receive a daily dose of SR141716 or vehicle.

Baseline BAT temperatures were similar in both groups and displayed the typical circadian profile with higher BAT temperatures in the dark period (ESM Fig. 2). SR141716 injection promptly increased BAT temperature within 1 h from the first dose (Fig. 4a) compared with the same time at baseline or with vehicle (average increase of 1.5°C). VEH mice showed no change in BAT temperature compared with baseline. The difference in iBAT temperature between the SR and VEH groups was greater in the light than in the dark phase of the cycle, perhaps because of the time of SR141716 delivery (12:00 hours in the light cycle). Although the magnitude of SR141716 effect on iBAT temperature was attenuated by day 10 (Fig. 4b), the AUC of

Fig. 4 SR141716 treatment induces BAT thermogenesis. iBAT temperature measurement with implantable probes during (a) the first 3 days and (b) the last 3 days of treatment with 10 mg/kg SR141716 i.p. (black squares) or vehicle (white squares). The shaded area indicates the dark period, while the vertical line indicates time of injection. **c** AUCs of iBAT temperature during days 1–3 and 10–12 in VEH (white bars) and SR (black bars). **d** Expression of *Pgc-1 α* , *Ucp1* and *Ppar δ* in iBAT from VEH (white bars), SR (black bars) and PF (hatched bars) groups. For **a–c**, $n=6$, and for **d**, $n=11$; $*p<0.05$ (SR group vs other groups on the same graph). a.u., arbitrary units



iBAT temperature for days 10 to 12 was still significantly elevated (Fig. 4c).

The strong thermogenic effect of SR141716 on BAT was accompanied by a significant increase in BAT expression of *Ucp1*, which encodes the uncoupling protein that mediates thermogenesis in BAT [21], and *Pgc-1 α* (also known as *Ppargc1a*) and *Ppar δ* (also known as *Ppard*), which encode the co-activator and transcription factor, respectively, that are implicated in the activation and differentiation of BAT [22] (Fig. 4d).

In a separate cohort, we examined the morphological changes induced by SR141716 in BAT (Fig. 5a,b). CB1 antagonism prominently increased the number of multilocular adipocytes, a typical feature of activated BAT.

Taken together these data indicate that CB1 antagonism causes a marked activation of BAT function.

SNS-dependent effects of CB1 antagonism on iBAT

To determine whether the effects of CB1 antagonism on BAT require the SNS, we surgically denervated the iBAT of DIO mice and tested the effect of CB1 antagonism on weight loss and BAT function. Successful denervation was verified by immunoblot (Fig. 5e) and immunohistochemistry (ESM Fig. 3a-f) using tyrosine hydroxylase as a marker of sympathetic nerve endings. Denervation dramatically altered BAT morphology, turning its lipid droplets from multilocular to unilocular (Fig. 5c), and SR141716 treatment did not

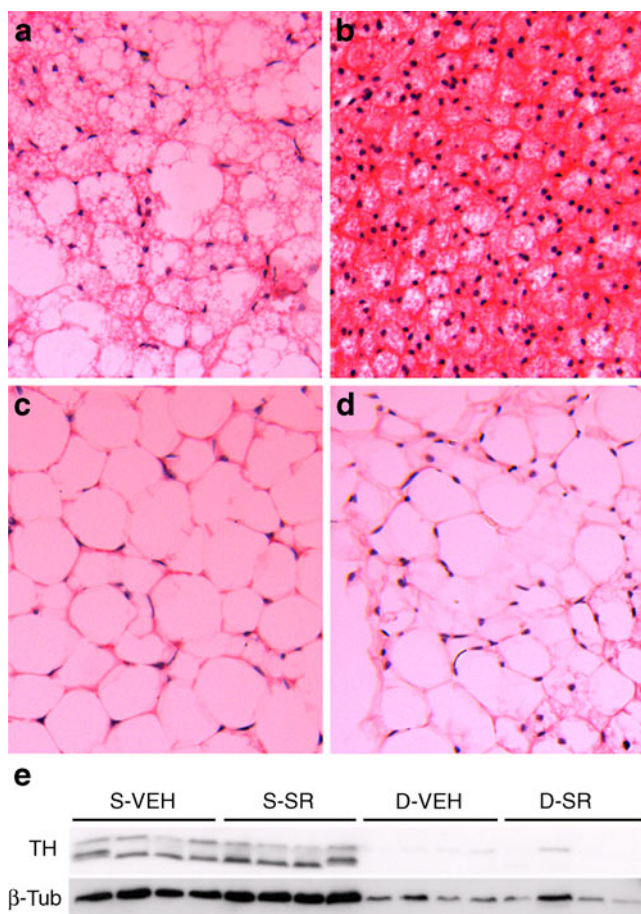


Fig. 5 Effect of CB1 antagonism on iBAT morphology in sham-operated or denervated mice. **a–d** Haematoxylin and eosin staining of iBAT after chronic treatment with 10 mg/kg SR (**b,d**) or vehicle (**a,c**) in sham-operated (**a,b**) and denervated (**c,d**) mice. In order to confirm effectiveness of the surgical denervation, tyrosine hydroxylase, a marker of SNS innervation, was measured by western blot (**e**). In all groups, $n=4$. D-VEH, denervated VEH group; D-SR, denervated SR group; S-SR, sham-operated SR group; S-VEH, sham-operated VEH group; β -Tub, β -tubulin; TH, tyrosine hydroxylase

significantly reverse this effect (Fig. 5d). Denervation of iBAT had no effect on body weight or fat mass in VEH or SR groups (Fig. 6a,b). However, denervation blunted the ability of SR141716 to increase insulin-stimulated glucose uptake (Fig. 6c). The expression of *Ucp1* was markedly downregulated by denervation and showed only a trend to be induced by SR independently of the SNS (Fig. 6d). On the other hand, *Pgc-1 α* levels were not regulated by denervation, which blunted the ability of SR to induce *Pgc-1 α* (Fig. 6e).

Discussion

In agreement with previous reports, we find that chronic CB1 antagonism reduces body weight because of both

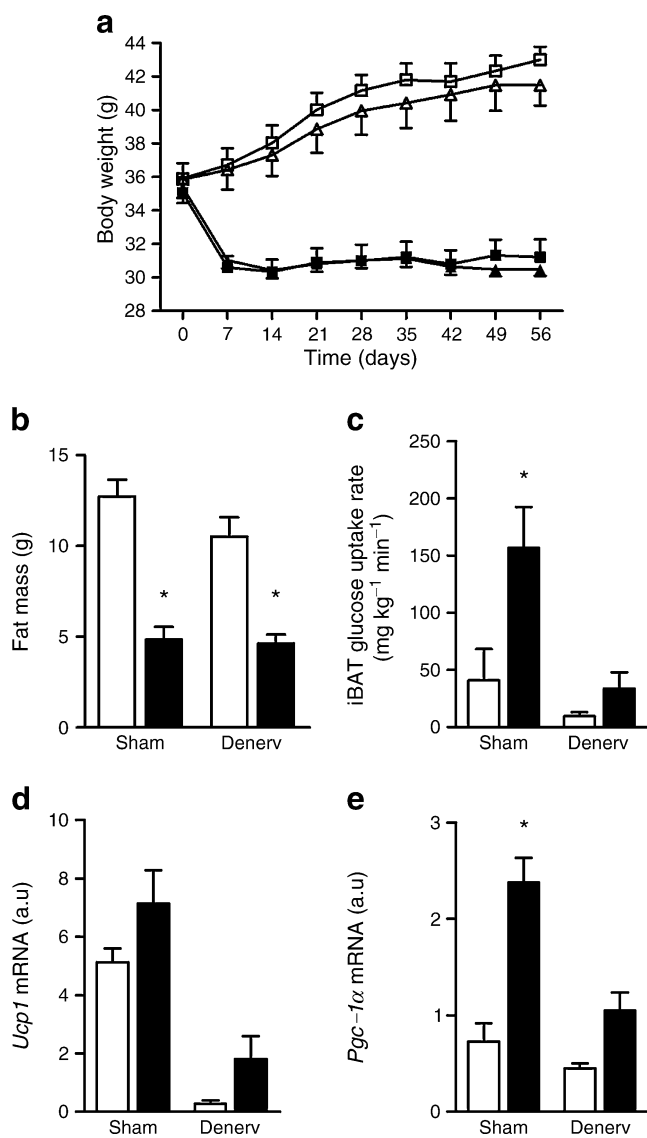


Fig. 6 Effect of denervation on body weight, adiposity and iBAT glucose uptake and gene expression. **a** Body weight of SR and VEH animals (black and white symbols, respectively) that had sham operation or iBAT denervation (squares and triangles, respectively). In **b–e**, white bars and black bars represent VEH and SR groups, respectively. **b** Fat mass of SR and VEH animals that had sham operation or iBAT denervation. **c–e** Activation of iBAT in sham-operated and denervated animals after chronic treatment with SR141716. **c** Glucose uptake in iBAT measured by 2-deoxy-[U- 14 C]glucose under hyperinsulinaemic conditions. **d** *Ucp1* mRNA expression (by two-way ANOVA: main effect of SR and denervation $p \leq 0.05$). **e** *Pgc-1 α* mRNA expression. For **a** and **b**, $n=13$ /group; for **c**, $n=8$ /group; and for **d** and **e**, $n=5$ /group; * $p < 0.05$ SR group vs VEH group. a.u., arbitrary units; Denerv, denervated

transient anorexia and, more importantly, increased energy expenditure [2].

Our data show that chronic SR141716 administration results in a significant increase in insulin-dependent glucose utilisation, including an increase in the rates of glycolysis and glycogen synthesis. In our experimental model of DIO, the effects of CB1 antagonism show an unexpected pattern

in the amelioration of specific components of insulin action. Although SR141716 treatment greatly increased insulin-dependent glucose utilisation, the rate of hepatic glucose production was not significantly changed, implying that CB1 antagonism cannot improve hepatic insulin resistance in DIO mice. This result is at odds with previous reports in which chronic SR141716 treatment elicited a significant improvement in hepatic insulin sensitivity [4, 5]. The effect of SR141716 on hepatic insulin sensitivity was shown to depend on increased levels of plasma adiponectin, whereas the effects of SR141716 on weight loss and glucose utilisation were not [5]. Indeed, several reports have implicated the endocannabinoid system as a modulator of adiponectin production and secretion [4, 5, 23–26]. This adipokine is known as a powerful inhibitor of hepatic glucose production [27, 28]. However, we and others could not detect changes in adiponectin levels (Table 1) [1, 29–31], which might explain why we did not detect an improvement in hepatic insulin sensitivity. The reasons for this lack of effect on adiponectin are not known and need further investigation.

An alternative explanation for the failure of SR141716 to decrease hepatic glucose production could be an inhibitory effect of dietary fat on insulin sensitivity. Indeed, we show that weight reduction by food restriction alone in our DIO mice fails to ameliorate *in vivo* insulin action, albeit these mice have a fat mass similar to that of SR141716-treated DIO mice (ESM Fig. 1). These results also suggest that the stimulatory effects of SR141716 on insulin-dependent glucose utilisation are specific to weight loss secondary to CB1 antagonism, as similar weight loss induced with food restriction does not restore insulin sensitivity (ESM Fig. 1). Since weight reduction does not always appear to lower endocannabinoid levels in obese individuals [32], we speculate that the beneficial effects of SR141716 on glucose metabolism are possibly secondary to the blockade of overstimulated CB1 receptors.

Another typical result of weight loss is an improvement in insulin-stimulated glucose uptake in skeletal muscle [33], which was not observed in our experiments with chronic administration of SR141716, nor was it observed in the food-restricted DIO mice. Our findings are in agreement with previous reports that did not observe a significant effect of SR141716 on insulin-stimulated glucose uptake in muscle of DIO mice [4, 5]. However, our studies did show significantly enhanced insulin-stimulated glycogen synthesis in skeletal muscle to an extent large enough to contribute significantly to the whole-body increase in glucose utilisation promoted by SR141716.

Notably, glycogen synthesis of skeletal muscle was increased in the absence of a significant stimulation of glucose uptake. Although the effect of insulin on glycogen stores is typically influenced by glucose transport, insulin can increase glycogen synthesis in muscle independently of

an increase in glucose uptake [34]. The effect of SR141716 on glycogen synthesis is not mediated by a change in glycogen phosphorylase or glycogen synthase (data not shown). Thus, CB1 antagonism may affect the activity of glycogen enzymes via alteration of transduction signalling or production of glycogen regulatory proteins. One possible explanation for the lack of a significant increase in glucose uptake in muscle is that CB1 antagonism increases fatty acid oxidation [6] which, in turn, can lead to inhibition of glucose uptake [35].

Unlike muscle, chronic CB1 antagonism strikingly increases insulin-stimulated glucose uptake of BAT. However, under basal conditions, chronic CB1 antagonism does not lead to an appreciable increase in BAT glucose uptake. This result indicates that chronic CB1 antagonism does not increase basal glucose uptake in BAT, suggesting that an SNS-dependent increase in BAT glucose uptake is not tonically stimulated. However, it reveals a novel role for CB1 receptors in the SNS as modulators of insulin action in BAT.

Denervation studies show that CB1-antagonist-mediated BAT differentiation and activation are strongly dependent on SNS innervation. Our data are in agreement with a report showing that CB1 antagonism in lean rats activates BAT in an SNS-dependent fashion [8]. Moreover, Quarta et al. have shown that BAT denervation blunts the enhancement of BAT glucose uptake after administration of SR141716 or exposure to cold [9]. Accordingly, we observed changes in histological, molecular and thermogenic variables after surgical denervation that indicate a substantial loss of function of BAT.

Interestingly, although the effects of SR141716 on BAT functions were blunted, iBAT denervation did not alter SR141716-mediated loss of body weight or fat mass, or energy expenditure. Previous studies on denervation or ablation of iBAT have yielded contrasting results with failure [36–38] and success [37] in altering body weight. Explanations for the failure are that the denervation of iBAT is limited to only 40% of total BAT mass. This may lead to compensatory activation of BAT in other fat depots, particularly as our studies were not conducted at thermoneutrality (ambient temperature 22°C). Nevertheless, these results point to a novel role for CB1 receptors in modulating BAT insulin sensitivity with SNS-dependent mechanisms. Although the complex interaction between the SNS and insulin action needs to be elucidated, we can speculate that CB1 signalling through the SNS is crucial for the modulation of BAT glucose and fat uptake. Indeed, the coordinated partitioning of these fuels plays an important role in BAT thermogenesis [39, 40].

It is important to note that the CB1 receptors responsible for modulating BAT function and thermogenesis may not be exclusively located in the central nervous system. In

support of this notion, peripheral but not central administration of SR141716 induced food-independent weight loss in DIO rats [6]. Also, peripherally restricted CB1 antagonists can cause substantial weight loss and increase energy expenditure [41]. Taken together, these data suggest the thermogenic effects of CB1 antagonism could involve peripheral mechanisms, including BAT activation.

In conclusion, our data show that CB1 antagonism markedly improves insulin-mediated glucose utilisation in DIO mice independent of its anorectic properties, via mechanisms that are not reproduced by food restriction alone. BAT is the major target organ for the effect of CB1 antagonism on insulin-dependent glucose uptake via a mechanism that requires an intact SNS. These novel data point to a crucial role of SNS CB1 receptors in modulating body weight and glucose metabolism through activation of BAT function.

Acknowledgements This work was supported by grants from the National Institutes of Health (DK078283), The American Diabetes Association (research grant 707RA11677), the Cincinnati Mouse Metabolic Phenotyping Center (MMPC DK59630) and Ethicon Endosurgery. Special thanks to S. Lipp and M. Fitzgerald for their outstanding technical assistance.

Contribution statement All authors substantially contributed to this work by participating in the design and analysis of the experiments, the drafting and revisions of the article and gave final approval of the published version.

Duality of interest M. Tschöp is a consultant for Roche Pharma and for Ambrx Inc. The remaining authors declare that they have no duality of interest associated with this manuscript.

References

- Cota D, Sandoval DA, Olivieri M et al (2009) Food intake-independent effects of CB1 antagonism on glucose and lipid metabolism. *Obesity (Silver Spring)* 17:1641–1645
- Herling AW, Kilp S, Elvert R, Haschke G, Kramer W (2008) Increased energy expenditure contributes more to the body weight-reducing effect of rimonabant than reduced food intake in candy-fed wistar rats. *Endocrinology* 149:2557–2566
- Ravinet TC, Delgorge C, Menet C, Arnone M, Soubrie P (2004) CB1 cannabinoid receptor knockout in mice leads to leanness, resistance to diet-induced obesity and enhanced leptin sensitivity. *Int J Obes Relat Metab Disord* 28:640–648
- Migrenne S, Lacombe A, Lefevre AL et al (2009) Adiponectin is required to mediate rimonabant-induced improvement of insulin sensitivity but not body weight loss in diet-induced obese mice. *Am J Physiol Regul Integr Comp Physiol* 296:R929–R935
- Watanabe T, Kubota N, Ohsugi M et al (2009) Rimonabant ameliorates insulin resistance via both adiponectin-dependent and adiponectin-independent pathways. *J Biol Chem* 284:1803–1812
- Nogueiras R, Veyrat-Durebex C, Suchanek PM et al (2008) Peripheral, but not central, CB1 antagonism provides food intake-independent metabolic benefits in diet-induced obese rats. *Diabetes* 57:2977–2991
- O'Hare JD, Zielinski E, Cheng B, Scherer T, Buettnner C (2011) Central endocannabinoid signaling regulates hepatic glucose production and systemic lipolysis. *Diabetes* 60:1055–1062
- Verty AN, Allen AM, Oldfield BJ (2009) The effects of rimonabant on brown adipose tissue in rat: implications for energy expenditure. *Obesity (Silver Spring)* 17:254–261
- Quarta C, Bellocchio L, Mancini G et al (2010) CB(1) signaling in forebrain and sympathetic neurons is a key determinant of endocannabinoid actions on energy balance. *Cell Metab* 11:273–285
- Virtanen KA, Lidell ME, Orava J et al (2009) Functional brown adipose tissue in healthy adults. *N Engl J Med* 360:1518–1525
- Cypess AM, Lehman S, Williams G et al (2009) Identification and importance of brown adipose tissue in adult humans. *N Engl J Med* 360:1509–1517
- Marken Lichtenbelt WD, Vanhommerig JW, Smulders NM et al (2009) Cold-activated brown adipose tissue in healthy men. *N Engl J Med* 360:1500–1508
- Liu YL, Connoley IP, Wilson CA, Stock MJ (2005) Effects of the cannabinoid CB1 receptor antagonist SR141716 on oxygen consumption and soleus muscle glucose uptake in Lep(ob)/Lep(ob) mice. *Int J Obes (Lond)* 29:183–187
- Rinaldi-Carmona M, Barth F, Heaulme M et al (1994) SR141716A, a potent and selective antagonist of the brain cannabinoid receptor. *FEBS Lett* 350:240–244
- Okamoto H, Obici S, Accili D, Rossetti L (2005) Restoration of liver insulin signaling in Insr knockout mice fails to normalize hepatic insulin action. *J Clin Invest* 115:1314–1322
- Lo CM, Obici S, Dong HH et al (2011) Impaired insulin secretion and enhanced insulin sensitivity in cholecystokinin-deficient mice. *Diabetes* 60:2000–2007
- Pfluger PT, Herranz D, Velasco-Miguel S, Serrano M, Tschöp MH (2008) Sirt1 protects against high-fat diet-induced metabolic damage. *Proc Natl Acad Sci USA* 105:9793–9798
- Massillon D, Chen W, Hawkins M, Liu R, Barzilai N, Rossetti L (1995) Quantitation of hepatic glucose fluxes and pathways of hepatic glycogen synthesis in conscious mice. *Am J Physiol* 269:E1037–E1043
- Rossetti L, Stenbit AE, Chen W et al (1997) Peripheral but not hepatic insulin resistance in mice with one disrupted allele of the glucose transporter type 4 (GLUT4) gene. *J Clin Invest* 100:1831–1839
- Brito MN, Brito NA, Baro DJ, Song CK, Bartness TJ (2007) Differential activation of the sympathetic innervation of adipose tissues by melanocortin receptor stimulation. *Endocrinology* 148:5339–5347
- Enerback S, Jacobsson A, Simpson EM et al (1997) Mice lacking mitochondrial uncoupling protein are cold-sensitive but not obese. *Nature* 387:90–94
- Kajimura S, Seale P, Spiegelman BM (2010) Transcriptional control of brown fat development. *Cell Metabolism* 11:257–262
- Despres JP, van Gaal L, Pi-Sunyer X, Scheen A (2008) Efficacy and safety of the weight-loss drug rimonabant. *Lancet* 371:555–557
- Jourdan T, Djaouti L, Demizieux L, Gresti J, Verges B, Degraze P (2010) CB1 antagonism exerts specific molecular effects on visceral and subcutaneous fat and reverses liver steatosis in diet-induced obese mice. *Diabetes* 59:926–934
- Poirier B, Bidouard JP, Cadrouvele C et al (2005) The anti-obesity effect of rimonabant is associated with an improved serum lipid profile. *Diabetes Obes Metab* 7:65–72
- Flamment M, Gueguen N, Wetterwald C, Simard G, Malthiery Y, Ducluzeau PH (2009) Effects of the cannabinoid CB1 antagonist,

- rimonabant, on hepatic mitochondrial function in rats fed a high fat diet. *Am J Physiol Endocrinol Metab* 297:E1004–E1012
27. Berg AH, Combs TP, Scherer PE (2002) ACRP30/adiponectin: an adipokine regulating glucose and lipid metabolism. *Trends Endocrinol Metab* 13:84–89
 28. Combs TP, Berg AH, Obici S, Scherer PE, Rossetti L (2001) Endogenous glucose production is inhibited by the adipose-derived protein Acrp30. *J Clin Invest* 108:1875–1881
 29. Pagano C, Pilon C, Calcagno A et al (2007) The endogenous cannabinoid system stimulates glucose uptake in human fat cells via phosphatidylinositol 3-kinase and calcium-dependent mechanisms. *J Clin Endocrinol Metab* 92:4810–4819
 30. Thornton-Jones ZD, Kennett GA, Benwell KR et al (2006) The cannabinoid CB1 receptor inverse agonist, rimonabant, modifies body weight and adiponectin function in diet-induced obese rats as a consequence of reduced food intake. *Pharmacol Biochem Behav* 84:353–359
 31. Bennetzen MF, Nielsen MP, Richelsen B, Pedersen SB (2008) Effects on food intake and blood lipids of cannabinoid receptor 1 antagonist treatment in lean rats. *Obesity (Silver Spring)* 16:2451–2455
 32. Engeli S, Bohnke J, Feldpausch M et al (2005) Activation of the peripheral endocannabinoid system in human obesity. *Diabetes* 54:2838–2843
 33. Friedman JE, Dohm GL, Leggett-Frazier N et al (1992) Restoration of insulin responsiveness in skeletal muscle of morbidly obese patients after weight loss. Effect on muscle glucose transport and glucose transporter GLUT4. *J Clin Invest* 89:701–705
 34. Rossetti L, Hu M (1993) Skeletal muscle glycogenolysis is more sensitive to insulin than is glucose transport/phosphorylation. Relation to the insulin-mediated inhibition of hepatic glucose production. *J Clin Invest* 92:2963–2974
 35. Randle PJ, Garland PB, Hales CN, Newsholme EA (1963) The glucose fatty-acid cycle. Its role in insulin sensitivity and the metabolic disturbances of diabetes mellitus. *Lancet* 1:785–789
 36. Rothwell NJ, Stock MJ (1989) Surgical removal of brown fat results in rapid and complete compensation by other depots. *Am J Physiol* 257:R253–R258
 37. Dulloo AG, Miller DS (1984) Energy balance following sympathetic denervation of brown adipose tissue. *Can J Physiol Pharmacol* 62:235–240
 38. Cox JE, Lorden JF (1986) Dietary obesity: brown fat denervation fails to alter development or recovery. *Am J Physiol* 250:R1108–R1116
 39. Yu XX, Lewin DA, Forrest W, Adams SH (2002) Cold elicits the simultaneous induction of fatty acid synthesis and beta-oxidation in murine brown adipose tissue: prediction from differential gene expression and confirmation in vivo. *FASEB J* 16:155–168
 40. Bartelt A, Bruns OT, Reimer R et al (2011) Brown adipose tissue activity controls triglyceride clearance. *Nat Med* 17:200–205
 41. Tam J, Vemuri VK, Liu J et al (2010) Peripheral CB1 cannabinoid receptor blockade improves cardiometabolic risk in mouse models of obesity. *J Clin Invest* 120:2953–2966